Available online at sjuoz.uoz.edu.krd

Science Journal of University of Zakho

Vol. 9, No. 4, pp. 184– 192, December-2021

p-ISSN: 2663-628X
e-ISSN: 2663-6298

journals.uoz.edu.krd

EFFECTS OF DEPOSITION TIME AND PH ON THE CHARACTERIZATION OF CHEMICALLY SYNTHESIZED COMPOSITE NANO-WIRES OF CU_2S THIN FILMS

Honar S. Ahmed [a,*], Raghad Y. Mohammed [a], Mohammed Hussein Khalil [a]

[a] Dept. of Physics, College of Science, University of Duhok, Duhok, Kurdistan Region , Iraq-(honar.salah, ssraghad and mohamadswary)@uod.ac

Received: Nov., 2021 / Accepted: Dec., 2021 / Published: Dec., 2021 *https://doi.org/10.25271/sjuoz.2021.9.4.863*

ABSTRACT:

The chemical bath deposition technique (CBD) had used for depositing Cu_2S thin films on the glass substrates. It found that thickness and deposition rate were significantly dependent on deposition parameters (deposition time and pH value). XRD data indicates that at different deposition times and pH values are given amorphous structure except for the deposited thin film of (8hours) and, pH of (10.4) the structure was crystalline. The morphology of the deposited thin films remarkably changed as the deposition time increased. Optical transmittance measurements illustrate that transmission of the thin films decreases from 93.27% for a deposition time of 4 hours to 81.73 for deposition time of 10 hours and, the maximum transmission rate of the films is 95.21 % with pH=8.4 and decreases to 28.39 % with pH=11.4. Also, optical studies revealed that Cu_2S thin film with direct energy bandgap decreased from 3.04 to 2.78 eV as deposition time increased and from 3.09 to 2.32 eV as pH increased.

KEYWORDS: Cu_2S thin film, CBD, Bandgap, thin-film, optical properties, XRD

1. INTRODUCTION

Nowadays, there is a huge increment in the study of nanoscale semiconducting materials due to the properties in nano shapes varying essentially from those of their bulk counterparts (Shinde et al., 2012). Besides nontoxic and abundant materials in the earth´s crust, such as the transition metal chalcogenides (sulfides, tellurides, and oxides), are critical of considering for the advancement of innovative materials. The investigation has extended due to their fabulous physical and chemical properties(CRUZ et al., 2012).

Cu_2S is a well-known material because of its significant optical and electrical properties which allow copper sulphide to be utilized in different important applications (Ismail et al., 2020) such as optoelectronic devices (Kim et al., 2017), absorbers for solar energy conversion (Ghdeeb, 2015), ion batteries and superconductors (Li et al., 2017; Liu et al., 2018), gas sensors (Sagade & Sharma, 2008), heterojunction photodetectors such as Cu2S/CdS, ZnO/Cu2S, Cu2S/ZnS and Cu2S/n-Si (Guo et al., 2014; Ismail et al., 2019; Zhan et al., 2020), and supercapacitors (Bulakhe et al., 2016).

The Cu_xS system has five stable phases: chalcocite (Cu_2S), djulerite ($Cu_{1.97}S$), digenite ($Cu_{1.8}S$), anilite ($Cu_{1.75}S$) ($Cu_{1.4}S$) and yarrowite ($Cu_{1.12}S$) these are referred to as blaubleibender covellite (CRUZ et al., 2012). copper sulphide could have a variety of crystal structures according to the value of X, such as orthorhombic, pseudo cubic, hexagonal, and tetragonal (Pathan & Lokhande, 2004). For instance, Cu_2S has a hexagonal structure, whereas Cu_2S could be found in both orthorhombic and hexagonal crystal structures (Buba & Adelabu, 2009). Cu_2S is a binary p-type Semiconductor with a bulk band gap of 1.2 eV (Ha et al., 2021). Many different techniques were used for the deposition of Cu_2S for example pulsed laser deposition (Maji et al., 2013), successive ionic layer absorption and reaction (SILAR)(Pathan et al., 2002), atomic layer deposition (Schneider et al., 2016), spray pyrolysis (Isac et al., 2007; Nho et al., 2012), chemical bath deposition (CBD) (Ishii et al., 1993; Ismail et al., 2020; Manjulavalli & Kannan, 2015; Muhammed et al., 2019), and photochemical deposition (Podder et al., 2005). The most popular thin films deposition technique is the chemical bath deposition (CBD) because it has many advantages over the other deposition techniques such as large deposited thin film area, cost-effective, low temperature and no high pressure or vacuum needed for the deposition process (OMWOYO, 2019). Besides, it has a limitation regarding the temperature of deposition. The temperature is normally restricted to about (100 °C), the inefficiency of the process, in terms of the utilization of starting materials and their conversion to thin films, the generation and disposal of large quantities of hazardous waste (Hodes, 2002; Lee, 2007), inadequate mixing of the reactants, and lack of control over reaction processing time (Kırmızıgül et al., 2013). Many parameters have to be noticed during the deposition process by CBD technique such as deposition time, bath temperature, pH value, and chemical reagents because they have a great effect on the deposited thin films' properties.

In this work, the CBD technique was utilized to deposit Cu_2S nanowire thin films on a glass substrate. Its structural, morphological, and optical properties have been examined concerning deposition parameters (time of deposition and pH value).

2. EXPERIMENT

Glass slides of the dimensions (25×75×1 mm) were used as substrates. Initially, the substrates were steeped for 24 hours in Chromic Acid to create nucleation sites in the glass substrates then washed in distilled water before being rinsed in Ethanol to

* Corresponding author

remove impurities on the glass substrate. Finally cleaned with distilled water and air-dried.

Analytical grade chemicals with purity (99.6%) copper (II) chloride dihydrate ($CuCl_2.2H_2O$) as a Cu^+ ions source, thiourea [SC $(NH_2)_2$] which represent a source of S^- ions with 15 % aqueous ammonia (NH_3) as a complexing agent were used for deposit Cu2S thin film. All chemicals were acquired from pro analysis ACS company. First, 50 ml of 0.2 M ($CuCl_2.2H_2O$) was mixed with an appropriate amount of a complexing agent which was (15 %) Ammonia solution to obtain the purposed pH of the solution. After a few minutes and under continuous stirring the solution becomes dark blue and uniform which indicates the copper's ions formation. After that 50 ml of 0.1M thiourea [SC $(NH_2)_2$] was added to the solution. The precleaned substrates were submerged vertically in the solution at room temperature (20ºC ± 2 ºC). The deposition process was executed at various deposition times 4,6,8 and 10 hours while other parameters kept constant (pH=10.4, $CuCl_2.2H_2O$ = 0.2 M, SC $(NH_2)_2$= 0.1 M) and different pH 8.4,9.4,10.4 and 11.4 while other parameters kept constant (Dt=8 hours, $CuCl_2.2H_2O$ conc. = 0.2 M, SC $(NH_2)_2$= 0.1 M). The different steps for the formation of Cu2S are shown in figure 1.

An optical interferometer technique was used for measuring Cu_2S thin film thickness. Where equation (1) was used for calculating the thickness of the deposited thin films.

$$d = \frac{\Delta x}{x}\frac{\lambda}{2} \qquad (1)$$

where
He-Ne laser wavelength (λ =632.8 nm), Δx is the distance between two fringes, and x is the width of the fringe (Chopra, 1969).

The X-Pert Pro PANalytical X-ray diffraction system was used to study the Structural properties of the Cu_2S thin films with CuKα radiation (1.5406 A°) in the 2θ range (10º-80º). The morphological properties of the surface of the Cu_2S thin films were studied by MIRA 3 TESCAN scanning electron microscopy (SEM). The optical transmission spectrums of the Cu_2S thin films were recorded by JENWAY 6850 UV/Vis spectrophotometer in the range of 350–1100 nm.

Tauc's equation was used to calculate the direct energy bandgap of the Cu_2S nanowires thin films (Makuła et al., 2018).

$$(\alpha h\nu)^2 = B(h\nu - Eg)^n \qquad (2)$$

where the bandgap energy (Eg), the transmittance (T), the absorption (A), the absorption coefficient (α) that is given by (α = 2.303 log (T/d)), is the incident photon energy (hυ), n depends on the transmission type (equals to 1/2 for allowed direct transmission and 2 for indirect transition),and the film thickness (d) (Makuła et al., 2018; Mohammed et al., 2020).

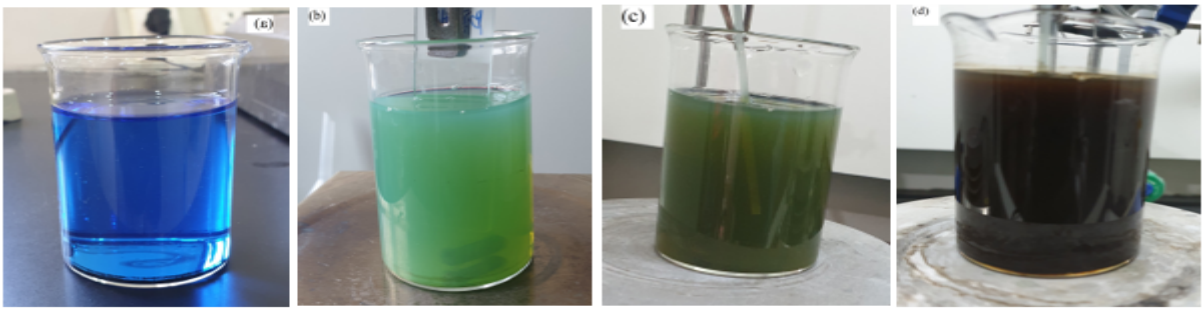

Figure 1. Changes of Chemical bath solution with time, where (a) mixture solution of $CuCl_2.2H_2O$, [SC $(NH_2)_2$], and NH_3. (b) after 2 min. (c) after 5-7 min. (d) after 20 min.

3. RESULTS AND DISCUSSION

3.1 Thickness and Growth rate

Thin film deposition occurs successfully when the ionic product transcends the solubility product of Cu_2S ($K_{sp} = 5 \times 10^{-48}$) and the bath solution becomes supersaturated. The precipitation begins with subsequent combinations of ions on the glass substrate surface and the formation of nuclei in solution (Offiah et al., 2012).
Figure . 2 shows the variation of Cu_2S nanowires thin films thickness with deposition time and pH value.

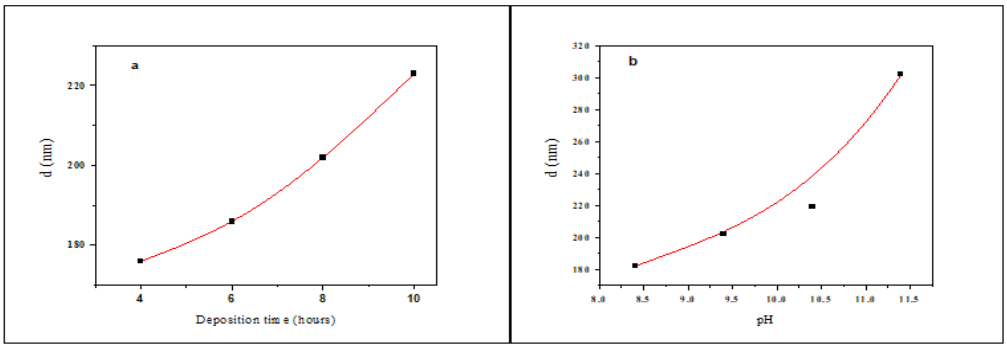

Figure 2. The variation of thickness of Cu_2S nanowires thin film with a) deposition time and, b) pH.

Figure 2a shows a smoothly increase of the thickness as the increasing of deposition time from 4 hrs. to 10hrs. The growth curve (figure 2a) reveals no thin film growth observed in the initial induction phase. The induction period then commences, followed by a systematic growth phase that begins with increasing film thickness as deposition time increases. This can also be deduced from the changing in the films' colour from grey colour for thickness(176nm) to dark grey for thickness(223nm). The thickness of the Cu_2S nanowires films with pH can be seen in figure 2b. It can be seen that the thickness increased from (182 to 302) nm when the pH value increased from (8.4 to 11.4). As observed in figure 2b, an increase in pH value leads to an increased growth rate. The reaction of thiourea hydrolysis will be pushed ahead this attributes due to the increase of OH^- ions concentration in the solution, increasing sulfide ion source generation, as shown in Eq. 4–5 (Vas-Umnuay & Chang, 2013):

$$(NH_2)_2CS + OH^- \leftrightarrow CH_2N_2 + H_2O + HS^- \quad (4)$$

$$HS^- \leftrightarrow S^{2-} + H^+ \quad (5)$$

There is no indication of saturation in both cases (Fig.2a and 2b). The variation of growth rate as a function of deposition time and pH value is shown in figure 3.

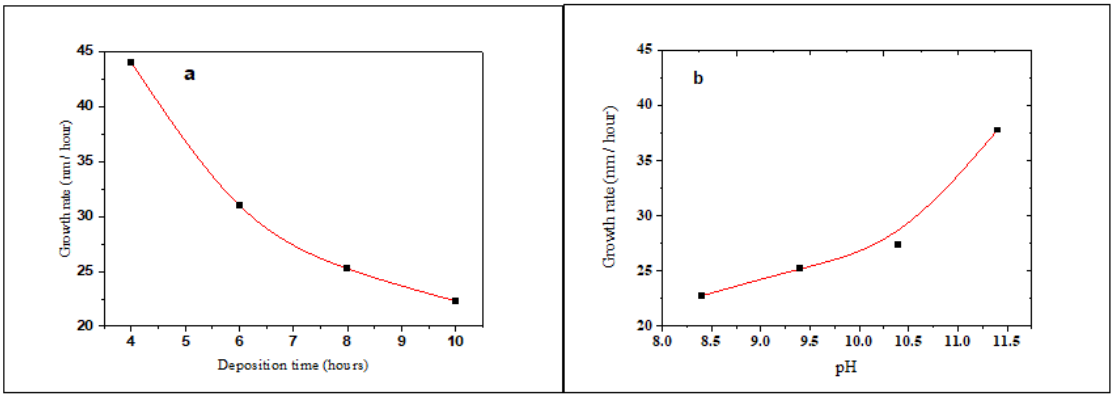

Figure 3. The variation of the growth rate of Cu_2S nanowires thin films with a) deposition times and, b) pH.

The growth rate decreased from (44 to 22.3 nm/hour) as the deposition time increased from (4 to 10 hours) as shown in figure 3a. This can be attributed to the precursor consumption over time (Mohammed et al., 2020). While in figure 3b. the growth rate increase from 22.75 nm/hour to 37.75 nm/hour as the pH increased from 8.4 to 11.4. This is because the concentration of OH^- ions increase in the solution, which accelerates the thiourea hydrolysis reaction. (Vas-Umnuay & Chang, 2013).

3.2 Structure properties of Cu_2S thin films

Figure 4. shows the XRD pattern of Cu2S thin films deposited at varied deposition times (4,6,8, and 10 hours).

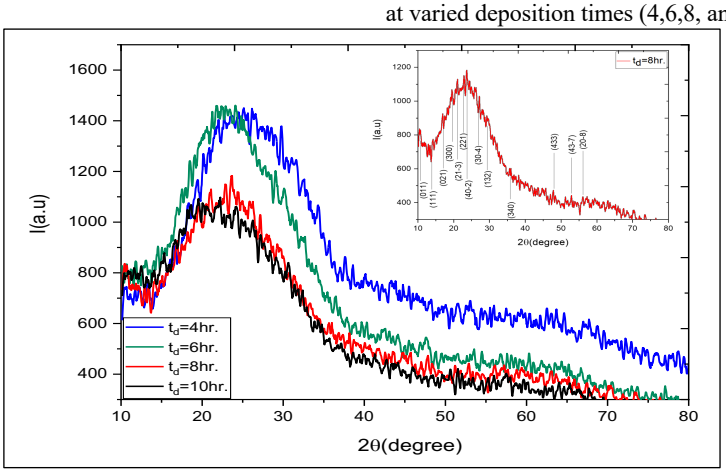

Figure 4. XRD pattern of Cu_2S nanowires thin films deposited at various deposition times at room temperature, pH= 10.4, $CuCl_2.2H_2O$ = 0.2 M and, $SC(NH_2)_2$= 0.1 M.

Figure 4. reveals that all deposited thin films give an amorphous structure except at a deposition time of 8 hours which is the optimum deposition time of Cu_2S nanowires thin film. It can be seen that the obtained XRD peaks of the diffraction patterns have been indexed as Cu_2S monoclinic-beta phase of copper sulfide according to the standard database spectrum (CPDS Card Code No. 829). In addition to that, no other peaks were detected from the other phases of copper sulfide, copper oxides, defects and impurities, which prove the high purity of the Cu_2S nanocrystal monoclinic-beta phase. Furthermore, it can be seen that their crystalline structure exhibits peaks corresponding to (011), (111), (021), (300), (21-3), (221), (40-2), (3 0 -4), (1 3 2) ,(340),(433),(43-7),and(20-8) planes. Figure 5. shows the Cu_2S thin films XRD pattern deposited at different pH values (8.4, 9.4, 10.4 and 11.4).

All deposited Cu_2S films give an amorphous structure in which no diffraction peaks are found in both spectra. However, increasing the pH of the bath solution leads to an increase in the crystallinity of the deposited films. But, increasing the pH to 11.4 results in the poor quality of the film's structure. The Cu_2S thin films deposited at pH = 10.4 had the corresponding optimum

crystallinity structure exhibits to the crystalline peaks that reported above . These patterns are in good agreement with earlier reported studies (Allouche et al., 2010). The broad hump in figures (4 and 5) is due to the glass substrate.

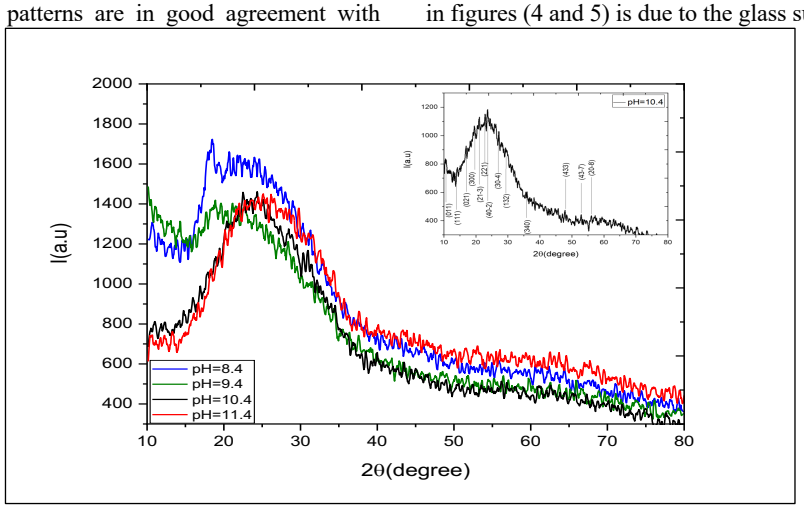

Figure 5. XRD pattern of deposited Cu_2S thin films at various pH values, constant bath temperature (room temperature), deposition time (8 hours), precursor concentration of ($CuCl_2.2H_2O$ = 0.2 M) and $SC(NH_2)_2$ = 0.1 M.

3.3 Morphological properties:

One of the most promising techniques for studying sample topography is a scanning electron microscope. Figure 6, shows the FESEM images of Cu_2S thin film deposited at different deposition times.

It can be seen from figure (6) that thin films are relatively well synthesized, homogeneous and uniformly covered with some cracks, compact and agglomerations inceased as deposition time increased. Besides, this indicates that more nucleation sites have been formed and the number of grains has increased. Also, one can notice that the deposited thin films morphology remarkably changed with the increase of the deposition time. Thin films deposited at (4, 6, and 10 hours) surface were covered with nanowires with average size (27.43, 35.18 and 27.6 nm) and a few nanoparticles with average size (30.14, 25.49 and 20.14), respectively. While thin film deposited at deposition time (8 hours) covered with nanoparticles with average size (30.36 nm).

Figure 7. shows the FESEM images of deposited films at various pH values. It is obvious from figure 6 that the Cu_2S thin films surface deposited at pH values (8.4, 9.4 and 11.4) covered with nanoparticles with average size (28.68, 30.69 and 33.61 nm). While, the Cu2S thin film surface deposited at pH value (10.4) is covered with nanowires and nanoparticles with average size (27.12 and 29,14), respectively. FESEM images confirmed that the agglomerations and the number of clusters increased as pH increased. An increasing of pH leads to the increase of OH^- ions which can cause noticeable morphological, shape changes and modify the repulsion and attraction forces. The increase of OH^- ions concentration pushes the reaction forward, weaken the repulsive forces, increase the attractive forces and allow the growth of oriented attachment (OA). when particles arrange perfectly with each other, the common boundary is eliminated, resulting to form the larger well-defined morphology particles (Xu et al., 2014; Yu et al., 2014), so the OA growth strongly depends on the pH (Reyes et al., 2018) as shown in figure 7.

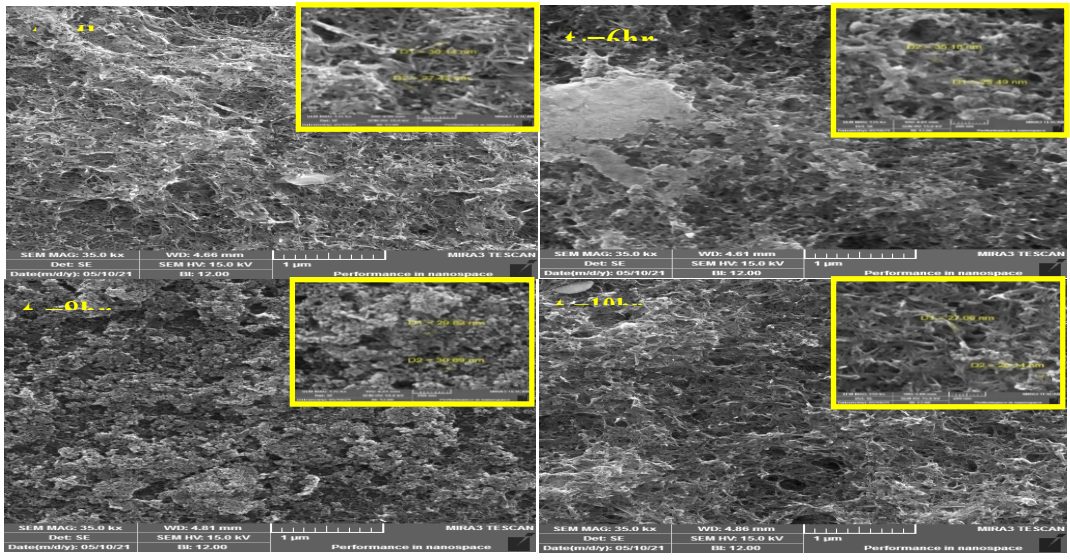

Figure 6. SEM images of Cu_2S films deposited at various deposition times at room temperature, pH= 10.4, $CuCl_2.2H_2O$ = 0.2 M, and $SC(NH_2)_2$ = 0.1 M.

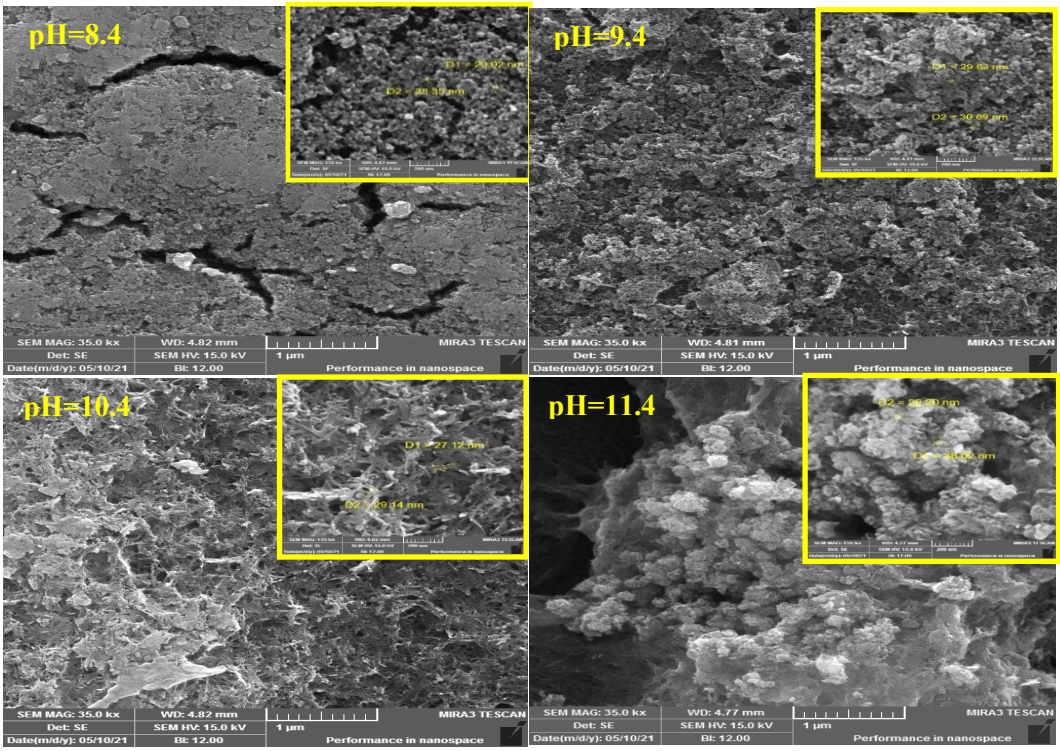

Figure 7. SEM images of Cu_2S films deposited at various pH values at room temperature, t_d=8 hours, $CuCl_2.2H_2O$ = 0.2 M, and $SC(NH_2)_2$ = 0.1 M.

3.4 Optical properties

3.4.1 Effect of deposition time: optical transmittance and absorbance spectra of Cu_2S thin films deposited at various deposition times can be seen in Figure 8.

From figure (8 a). according to the absorbance measurements of the films weak absorption is observed at longer wavelengths whereas high absorption is acquired at shorter wavelengths (UV-VIS). The absorption of the thin films increased as wavelength decreased to visible and NIR region. This makes the films to be suitable for use as thin coatings on windows to control the amount of light that enters a building and also reflect as much infrared radiation as possible. While, from figure (8b), one can see that the transmission of the thin films decreases from 93.27% for a deposition time of 4 hours to 81.73% for deposition time of 10 hours and this is attributed due to the increase in the films' thickness (Ghdeeb, 2015). Increasing the thickness of (Cu_2S) thin films leads to an increase in the depth of donor levels associated with these vacancies increases which cause these levels to be available for photons to be absorbed. As a result, the absorbance of Cu_2S thin films increases as well. figure (9) shows the absorption coefficient of Cu_2S thin films versus wavelength for different deposition times.

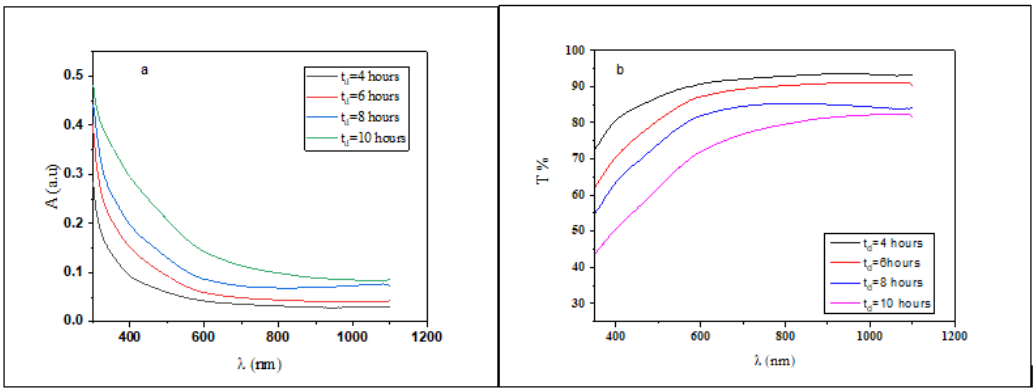

figure -8 a: Absorption spectrums of Cu_2S thin films at various deposition times versus wavelength b: transmission spectrums of Cu_2S thin films at various deposition times versus wavelength with pH=10.4, $CuCl_2.2H_2O$ = 0.2 M, and $SC(NH_2)_2$ = 0.1 M.

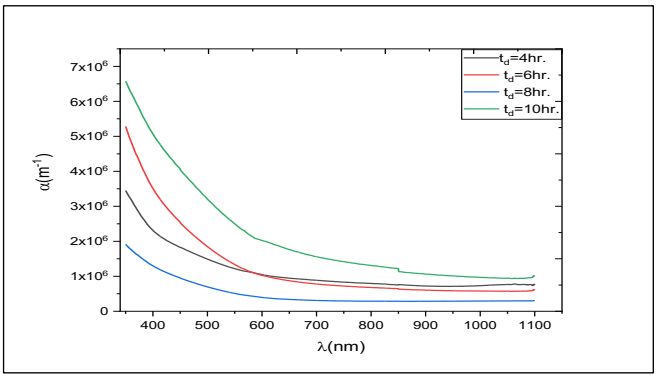

Figure -9 Absorption coefficient of Cu_2S thin films versus wavelength with pH=10.4, $CuCl_2.2H_2O$ = 0.2 M, and $SC(NH_2)_2$ = 0.1 M.

The high absorption coefficient of Cu_2S thin films (~2 $\times 10^6$- 6.5 $\times 10^6$ m^{-1}) for deposition time of 4 hours to 10 hours, indicates the direct transition band gap of the films (Ismail et al., 2019). The direct energy band gap of Cu_2S thin films was calculated from the plot of $(\alpha h\upsilon)^2$ versus $(h\upsilon)$ as shown in figure 10. Increasing the deposition time from 4 to 10 hours cause a reduction in the energy bandgap from 3.04 to 2.78 eV and this is shown in figure 11. These decrease in the energy gap of the Cu_2S thin films may be attributed due to the transition from a poor crystalline to a polycrystalline state (Kırmızıgül et al., 2013) or the film composition (Isac et al., 2013). The obtained energy gap values are approximately the same values obtained by (Ismail et al., 2020).

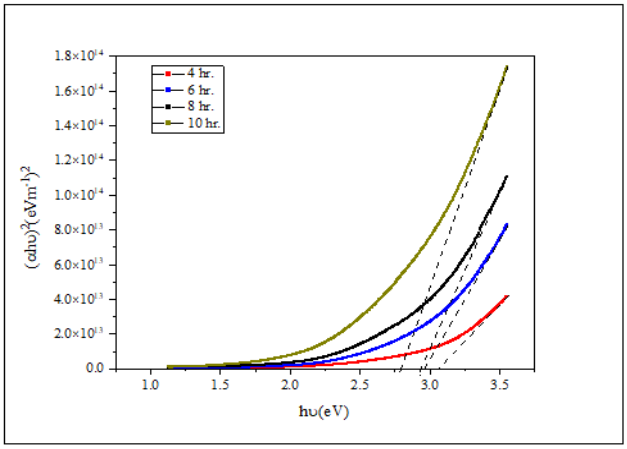

Figure 10. $(\alpha h\upsilon)^2$ with $(h\upsilon)$ at various deposition times (4,6,8 and 10 hours) at pH=10.4, $CuCl_2.2H_2O$ = 0.2 M, and $SC(NH_2)_2$= 0.1 M.

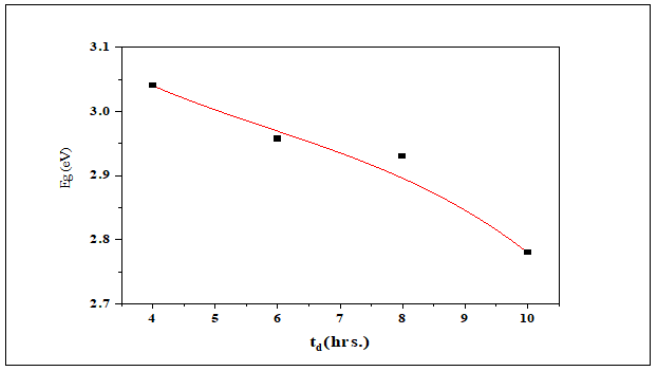

Figure 11. the variation of energy band gap of Cu_2S thin film with deposition times (4,6,8 and 10 hours) at pH=10.4, $CuCl_2.2H_2O$ = 0.2 M, and $SC(NH_2)_2$= 0.1 M.

3.4.2 Effect of pH: the effect of the various pH values of the bath solution on the Cu_2S thin films' transmission and absorbance spectracan be seen figure 12. Optical transmittance measurements illustrate that the maximum transmission rate of the films is 95.21 % with pH=8.4 and decreases to 28.39 % with pH=11.4 in the visible range. The decrease of transmission is due to the increase in films thickness

(Ghdeeb, 2015). While the absorption is 8.47 % for pH=11.4 and decreased to 1.6 % for pH =8.4 in the visible range.

Figure (13) shows the absorption coefficient of Cu_2S thin films versus wavelength for different pH growth condition.

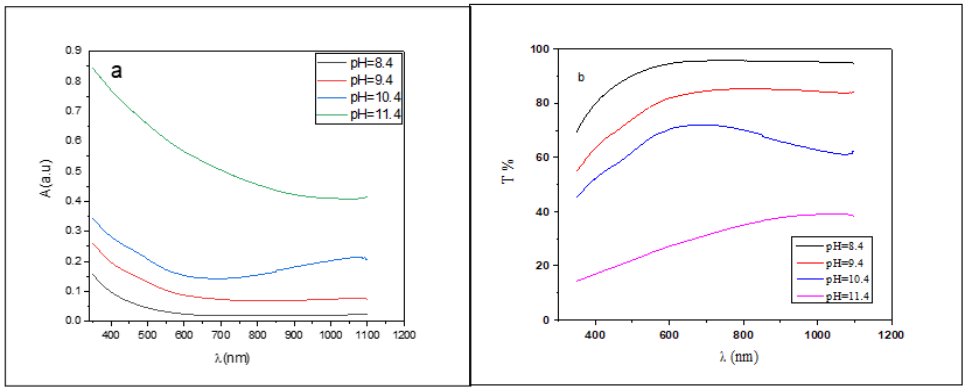

Figure 12. (a) absorption spectrums of Cu_2S thin films at various pH values versus wavelength (b) l transmission spectrums of Cu_2S thin films at various pH values versus wavelength with t_d=8hours, $CuCl_2.2H_2O$ = 0.2 M, and $SC(NH_2)_2$= 0.1 M.

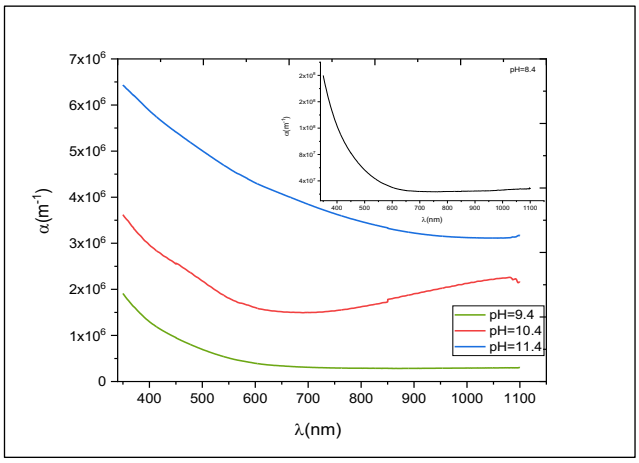

Figure -13 Absorption coefficient of Cu_2S thin films versus wavelength at different pH with t_d=8hours, $CuCl_2.2H_2O$ = 0.2 M, and $[SC(NH_2)_2$= 0.1 M.

The high absorption coefficient of Cu_2S thin films (~1.999×10^8-6.435×10^6 m^{-1}) for pH=8.4 to pH=11.4, indicates again the direct transition band gap of the thin films (Ismail et al., 2019).

According to the acquired measurements of optical transmission, The direct energy band gap of the Cu_2S thin films was calculated from the plot of $(\alpha h\upsilon)^2$ versus $(h\upsilon)$ as shown in figure 14.

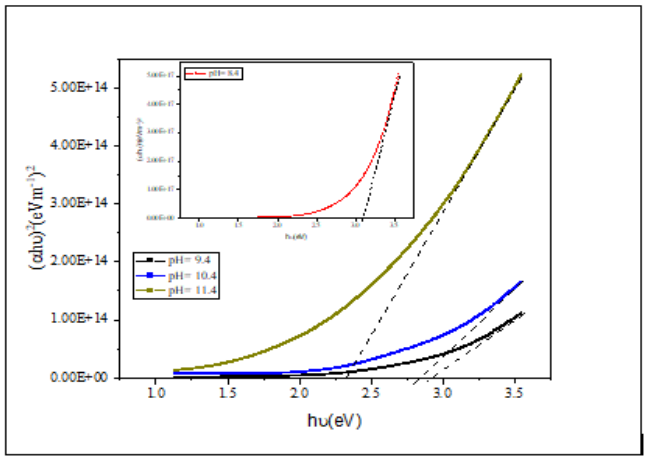

Figure -14 $(\alpha h\upsilon)^2$ with $(h\upsilon)$ of various pH values with t_d=8hours, $CuCl_2.2H_2O$ = 0.2 M, and $SC(NH_2)_2$= 0.1 M.

The result is a sharp optical absorption characteristic, showing homogeneous grain in shape and size and also low defect density towards the band edge. As can be seen in figure 15, $(\alpha h\upsilon)^2$ alters smoothly with $(h\upsilon)$ above the bandgap energy (Eg).

The Eg of Cu_2S thin films reduced from (3.02 to 2.32 eV) as pH raised from 8.4 to 11.4 as shown in figure 15. The obtaine Eg values slightly larger than obtained by (Muhammed et al., 2019). This shift in the energy band gap my be attribute due to quantum size effect exhibited by the nanocrystals present in Cu_2S film (Hone & Dejene, 2019; Kotadiya et al., 2012).

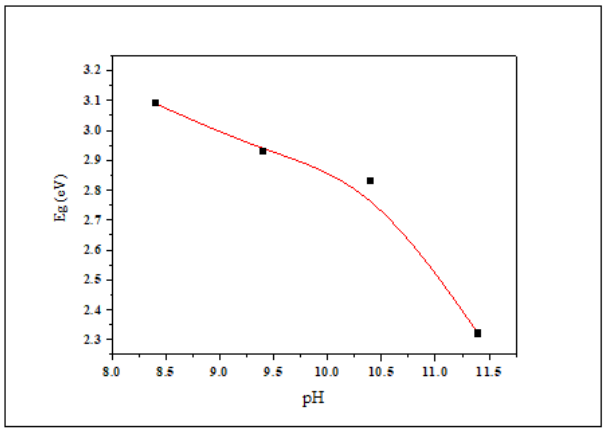

Figure -15 the variation of energy band gap of Cu_2S thin film with different pH at t_d=8hours, $CuCl_2.2H_2O$ = 0.2 M, and $SC(NH_2)_2$= 0.1 M.

4. CONCLUSION

Cu_2S thin films were deposited on glass substrates by the chemical bath deposition technique. The thickness of the deposited Cu_2S films increases as the deposition time and pH increase. The growth rate decreased with deposition time and increased as pH increased. The XRD results reveal that deposited thin films give an amorphous structure except at a deposition time of 8 hours. Cu_2S thin films were obtained at pH = 10. 4 had the best crystallinity and decreases when the pH increases to 11.4.
It can be seen that from SEM images, the thin films are relatively well synthesized, homogeneous and uniformly covered with some cracks and compact and agglomerations were inceased.The surface of the films is covered with nanowires and a few nanoparticles.

Optical measurement illustrates that the transmission of the Cu_2S thin films decreased with increasing pH and deposition time. The films' transparency increased as wavelength decreased from NIR to UV region. This makes the films be suitable as thin coatings on windows for warm climates. Increasing deposition time and pH leads to a reduction in the optical energy bandgap.

ACKNOWLEDGEMENTS

The authors are thankful to the University of Duhok for thier support.

REFERENCES

Allouche, N. K., Nasr, T. B., Guasch, C., & Turki, N. K. (2010). Optimization of the synthesis and characterizations of chemical bath deposited Cu2S thin films. *Comptes Rendus Chimie*, *13*(11), 1364-1369.

Buba, A., & Adelabu, J. (2009). Electrical Conductivity of CUXS Thin Film Deposited by Chemical Bath Deposition (CBD) Technique. *Nigerian Journal of Basic and Applied Sciences*, *17*(2), 161-165.

Bulakhe, R. N., Sahoo, S., Nguyen, T. T., Lokhande, C. D., Roh, C., Lee, Y. R., & Shim, J.-J. (2016). Chemical synthesis of 3D copper sulfide with different morphologies for high performance supercapacitors application. *RSC advances*, *6*(18), 14844-14851.

Chopra, K. L. (1969). Thin film phenomena.

CRUZ, J. S., HERNÁNDEZ, S. M., & CORONEL, J. (2012). Characterization of CuxS thin films obtained by CBD technique at differents annealing temperatures. *Chalcogenide Letters*, *9*(2), 85-91.

Ghdeeb, N. J. (2015). The effect of thickness on the optical properties of Cu2S thin films. *Iraqi Journal of Physics (IJP)*, *13*(26), 121-127.

Guo, K., Chen, X., Han, J., & Liu, Z. (2014). Synthesis of ZnO/Cu 2 S core/shell nanorods and their enhanced photoelectric performance. *Journal of sol-gel science and technology*, *72*(1), 92-99.

Ha, E., Xin, Z., Li, D., Zhang, J., Ji, T., Hu, X., Wang, L., & Hu, J. (2021). Dual-Modified Cu2S with MoS2 and Reduced Graphene Oxides as Efficient Photocatalysts for H2 Evolution Reaction. *Catalysts*, *11*(11), 1278.

Hodes, G. (2002). *Chemical solution deposition of semiconductor films*. CRC press.

Hone, F. G., & Dejene, F. B. (2019). Cationic concentration and pH effect on the structural, morphological and optical band gap of chemically synthesized lead sulfide thin films. *Journal of Materials Research and Technology*, *8*(1), 467-474.

Isac, L., Andronic, L., Enesca, A., & Duta, A. (2013). Copper sulfide films obtained by spray pyrolysis for dyes photodegradation under visible light irradiation. *Journal of Photochemistry and Photobiology A: Chemistry*, *252*, 53-59.

Isac, L., Duta, A., Kriza, A., Nanu, M., & Schoonman, J. (2007). Crystal order in Cu2S thin films obtained by spray pyrolysis. *Journal of optoelectronics and advanced materials*, *9*(5), 1265-1268.

Ishii, M., Shibata, K., & Nozaki, H. (1993). Anion distributions and phase transitions in CuS1-xSex (x= 0-1) studied by Raman spectroscopy. *Journal of Solid State Chemistry*, *105*(2), 504-511.

Ismail, R. A., Al-Samarai, A.-M. E., & Muhammed, A. M. (2019). High-performance nanostructured p-Cu 2 S/n-Si photodetector prepared by chemical bath deposition technique. *Journal of Materials Science: Materials in Electronics*, *30*(12), 11807-11818.

Ismail, R. A., Al-Samarai, A. M. E., & Ali, A. M. M. (2020). Effect of molar concentration of CuCl 2 on the characteristics of Cu 2 S film. *Optical and Quantum Electronics*, *52*(11), 1-14.

Kim, H.-J., Ko, B., Gopi, C. V., Venkata-Haritha, M., & Lee, Y.-S. (2017). Facile synthesis of morphology dependent CuS nanoparticle thin film as a highly efficient counter electrode for quantum dot-sensitized solar cells. *Journal of Electroanalytical Chemistry*, *791*, 95-102.

Kırmızıgül, F., Güneri, E., & Gümüş, C. (2013). Effects of different deposition conditions on the properties of Cu2S thin films. *Philosophical Magazine*, *93*(5), 511-523.

Kotadiya, N. B., Kothari, A. J., Tiwari, D., & Chaudhuri, T. K. (2012). Photoconducting nanocrystalline lead sulphide thin films obtained by chemical bath deposition. *Applied Physics A*, *108*(4), 819-824.

Lee, J.-H. (2007). Influence of substrates on the structural and optical properties of chemically deposited CdS films. *Thin Solid Films*, *515*(15), 6089-6093.

Li, H., Wang, Y., Jiang, J., Zhang, Y., Peng, Y., & Zhao, J. (2017). CuS microspheres as high-performance anode material for Na-ion batteries. *Electrochimica Acta*, *247*, 851-859.

Liu, Y., Zhou, Z., Zhang, S., Luo, W., & Zhang, G. (2018). Controllable synthesis of CuS hollow microflowers hierarchical structures for asymmetric supercapacitors. *Applied Surface Science*, *442*, 711-719.

Maji, S. K., Dutta, A. K., Bhadu, G. R., Paul, P., Mondal, A., & Adhikary, B. (2013). A novel amperometric biosensor for hydrogen peroxide and glucose based on cuprous sulfide nanoplates. *Journal of Materials Chemistry B*, *1*(33), 4127-4134.

Makuła, P., Pacia, M., & Macyk, W. (2018). How to correctly determine the band gap energy of modified semiconductor photocatalysts based on UV–Vis spectra. In: ACS Publications.

Manjulavalli, T., & Kannan, A. (2015). Effects of deposition time on structural, optical and electrical properties of chemically deposited Cu2S thin films. *J. Chem. Tech. Res*, *8*(11), 607-616.

Mohammed, K. A., Ahmed, S. M., & Mohammed, R. Y. (2020). Investigation of Structure, Optical, and Electrical Properties of CuS Thin Films by CBD Technique. *Crystals*, *10*(8), 684.

Muhammed, A. M., Ibrahim, A. E., & Ismail, R. A. (2019). Study an Effect of Thiourea Concentration on the Structural, Optical and Electrical Properties of (Cu2S) film Prepared by Chemical Bath Deposition (CBD). *Kirkuk University Journal-Scientific Studies*, *14*(3), 97-115.

Nho, P., Ngan, P., Tien, N., & Viet, H. (2012). Preparation and characterization of low resistivity CuS films using spray pyrolysis. *Chalcogenide Letters*, *9*(10), 397-402.

Offiah, S., Ugwoke, P., Ekwealor, A., Ezugwu, S., Osuji, R., & Ezema, F. (2012). Structural and spectral analysis of chemical bath deposited copper sulfide thin films for solar energy conversions. *Digest Journal of Nanomaterials and Biostructures*, *7*(1), 165-173.

OMWOYO, J. G. (2019). *CHARACTERIZATION OF Cu2S/SnO2: F PN JUNCTION FOR SOLAR CELL APPLICATIONS* KENYATTA UNIVERSITY].

Pathan, H., Desai, J., & Lokhande, C. (2002). Modified chemical deposition and physico-chemical properties of copper sulphide (Cu2S) thin films. *Applied Surface Science*, *202*(1-2), 47-56.

Pathan, H., & Lokhande, C. (2004). Deposition of metal chalcogenide thin films by successive ionic layer adsorption and reaction (SILAR) method. *Bulletin of Materials Science*, *27*(2), 85-111.

Podder, J., Kobayashi, R., & Ichimura, M. (2005). Photochemical deposition of CuxS thin films from aqueous solutions. *Thin Solid Films*, *472*(1-2), 71-75.

Reyes, O., Maldonado, D., Escorcia-García, J., & Sebastian, P. (2018). Effect of temperature and pH on direct chemical bath deposition of cuprous oxide thin films. *Journal of Materials Science: Materials in Electronics*, *29*(18), 15535-15545.

Sagade, A. A., & Sharma, R. (2008). Copper sulphide (CuxS) as an ammonia gas sensor working at room temperature. *Sensors and Actuators B: Chemical*, *133*(1), 135-143.

Schneider, N., Lincot, D., & Donsanti, F. (2016). Atomic layer deposition of copper sulfide thin films. *Thin Solid Films*, *600*, 103-108.

Shinde, M., Ahirrao, P., Patil, I., & Patil, R. (2012). Thickness dependent electrical and optical properties of nanocrystalline copper sulphide thin films grown by simple chemical route.

Vas-Umnuay, P., & Chang, C.-h. (2013). Growth kinetics of copper sulfide thin films by chemical bath deposition. *ECS Journal of Solid State Science and Technology*, *2*(4), P120.

Xu, H., Dong, J., & Chen, C. (2014). One-step chemical bath deposition and photocatalytic activity of Cu2O thin films with orientation and size controlled by a chelating agent. *Materials Chemistry and Physics*, *143*(2), 713-719.

Yu, M., Draskovic, T. I., & Wu, Y. (2014). Understanding the crystallization mechanism of delafossite CuGaO2 for controlled hydrothermal synthesis of nanoparticles and nanoplates. *Inorganic chemistry*, *53*(11), 5845-5851.

Zhan, Y., Shao, Z., Jiang, T., Ye, J., Wu, X., Zhang, B., Ding, K., Wu, D., & Jie, J. (2020). Cation exchange synthesis of two-dimensional vertical Cu 2 S/CdS heterojunctions for photovoltaic device applications. *Journal of Materials Chemistry A*, *8*(2), 789-796.